The Journal of Chemical Physics ARTICLE scitation.org/journal/jcp

Impurity incorporation and exchange interactions in Co^{2+}-doped CdSe/CdS core/shell nanoplatelets

Cite as: J. Chem. Phys. 151, 224708 (2019); doi: 10.1063/1.5129391
Submitted: 28 September 2019 • Accepted: 19 November 2019 •
Published Online: 13 December 2019

View Online Export Citation CrossMark

Rachel Fainblat,[1] Savas Delikanli,[2,3] Leon Spee,[1] Tamara Czerny,[1] Furkan Isik,[3] Vijay Kumar Sharma,[2] Hilmi Volkan Demir,[2,3] and Gerd Bacher[1,a)]

AFFILIATIONS

[1]Werkstoffe der Elektrotechnik and CENIDE, University of Duisburg-Essen, Bismarckstr. 81, Duisburg 47057, Germany
[2]Luminous! Center of Excellence for Semiconductor Lighting and Displays, School of Electrical and Electronic Engineering, School of Physical and Materials Sciences, School of Materials Sciences and Engineering, Nanyang Technological University, 639798, Singapore
[3]Department of Electrical and Electronics Engineering, Department of Physics, UNAM-Institute of Materials Science and Nanotechnology, Bilkent University, Ankara 06800, Turkey

Note: This paper is part of the JCP Special Topic on Colloidal Quantum Dots.
[a)]**Author to whom correspondence should be addressed:** gerd.bacher@uni-due.de

ABSTRACT

The intentional incorporation of transition metal impurities into colloidal semiconductor nanocrystals allows an extension of the host material's functionality. While dopant incorporation has been extensively investigated in zero-dimensional quantum dots, the substitutional replacement of atoms in two-dimensional (2D) nanostructures by magnetic dopants has been reported only recently. Here, we demonstrate the successful incorporation of Co^{2+} ions into the shell of CdSe/CdS core/shell nanoplatelets, using these ions (i) as microscopic probes for gaining distinct structural insights and (ii) to enhance the magneto-optical functionality of the host material. Analyzing interatomic Co^{2+} ligand field transitions, we conclude that Co^{2+} is incorporated into lattice sites of the CdS shell, and effects such as diffusion of dopants into the CdSe core or diffusion of the dopants out of the heterostructure causing self-purification play a minor role. Taking advantage of the absorption-based technique of magnetic circular dichroism, we directly prove the presence of *sp-d* exchange interactions between the dopants and the band charge carriers in CdSe/Co^{2+}:CdS heteronanoplatelets. Thus, our study not only demonstrates magneto-optical functionality in 2D nanocrystals by Co^{2+} doping but also shows that a careful choice of the dopant type paves the way for a more detailed understanding of the impurity incorporation process into these novel 2D colloidal materials.

Published under license by AIP Publishing. https://doi.org/10.1063/1.5129391

INTRODUCTION

The development of colloidal nanoplatelets (NPLs) started more than a decade ago when researchers adapted and expanded the protocols used for the fabrication of zero-dimensional (0D) II–VI nanocrystals.[1] Compared to 0D systems, two-dimensional (2D) NPLs offer great advantages such as the control of the quantum confinement at the monolayer (ML) level, narrower emission linewidths, shorter recombination lifetimes, directed emission, and larger absorption cross sections and coefficients.[2–8] In contrast to quantum dots, where absorption and/or emission energies can be continuously tuned,[9–11] the discrete change in ML thickness and thus in quantum confinement allows for a stepwise shift of the optical resonances. Colloidal atomic layer deposition (c-ALD) has been applied in the synthesis of complex core/shell (shell grown on top of a NPL core)[12,13] and core/crown (crown grown laterally around a NPL core)[14,15] heterostructures, finally enabling absorption and emission energies to be tuned via the delocalization of charge carrier wave functions.[16–18] Additionally, compared to core-only NPLs, 2D heterostructures exhibit reduced photoluminescence blinking

Published under license by AIP Publishing

and enhanced photoluminescence quantum yields,[14,19] thus triggering their implementation in optoelectronic devices such as light emitting diodes.[20–22] Even lasing after optical pumping has been demonstrated.[23–25]

Doping, i.e., the intentional incorporation of impurities into a crystal lattice, has been employed as a powerful strategy to tune optical, electrical, and magnetic properties of II–VI based zero-dimensional colloidal nanostructures,[26–35] even down to the level of magic-sized or molecular nanocluster.[36–41] In contrast to the sophisticated chemical routes reported for the synthesis of doped 0D nanocrystals, the incorporation of impurities into their 2D analogs is at an early stage of development. Via postsynthetic cation exchange, researchers have shown that Cd^{2+} can be replaced by copper and silver ions in CdSe NPLs.[42–44] However, the incorporation of further transition metal ions into core-only NPLs has not yet been reported. In the case of core/shell NPLs, Mn^{2+} doped CdS layers were grown on top of undoped CdSe NPLs via c-ALD.[45] Making deliberate use of the overlap between the partially delocalized charge carrier wave functions and the dopants inside the shell, clear signatures of *sp-d* exchange interactions were observed experimentally.[45–47] By changing the detailed architecture of the core/shell NPLs, tunability of both *s-d* and *p-d* exchange interactions has been achieved.[47]

More than endowing the host material with new functionalities, impurities can also be used as microscopic tools to investigate fundamental properties such as lattice parameters, thermal expansion, the presence of strain, and electron-phonon coupling.[41,48–50] For this purpose, impurities with a high crystal field sensitivity should be chosen, which are able to disclose small changes of their environment.[51] One example of this type of impurity is Co^{2+}, which exhibits well-defined ligand-field transitions in the visible and infrared spectral range.[52] Additionally, (magneto-) optical signatures of dopants can also reveal effects related to the incorporation of impurities into a crystal lattice such as ion diffusion and/or self-purification.[53] These basic concepts can be used as a powerful and versatile tool in the fast developing field of colloidal 2D nanostructures, allowing researchers to gain insight into structural properties and to understand the impurity incorporation process in these novel materials in more detail.

In this work, we took advantage of Co^{2+} ions as microscopic probes to demonstrate the successful incorporation of impurities into the shell of CdSe/CdS core/shell nanoplatelets (NPLs). The interatomic Co^{2+} ligand field (LF) absorption bands were used to investigate possible diffusion/segregation effects. Magnetic circular dichroism (MCD) spectroscopy has been applied to directly probe the exchange coupling between magnetic dopants with the band charge carriers in CdSe/Co^{2+}:CdS NPLs. The temperature dependence of the MCD signal indicates the absence of Co^{2+} clusters, showing the homogeneity of the doping process via colloidal atomic layer deposition.

RESULTS AND DISCUSSION

CdSe/Co^{2+}:CdS core/shell nanoplatelets (NPLs) were synthesized via colloidal chemistry routes and finally dispersed in hexane (the detailed synthesis procedure is described in the "Methods" section). In the first synthesis step, CdSe cores with a thickness of two monolayers (2 ML) were fabricated. These undoped cores were subsequently coated with a shell using colloidal atomic layer deposition (c-ALD). In each step of the shell growth via c-ALD deposition, both sides of the CdSe NPL surface were coated with 1 ML of shell material (either pure CdS or Co^{2+}:CdS), thus resulting in a total deposition of 2 ML (1 ML on the top and the bottom surface, respectively). In this work, we focused on the investigation of the (magneto-) optical properties of CdSe/Co^{2+}:CdS NPLs of three different shell thicknesses (3 ML, 4 ML or 5 ML on each, top and bottom surface, corresponding to a total thickness of 6 ML, 8 ML and 10 ML, respectively). The samples are denoted as (2)CdSe/(6)Co^{2+}:CdS, (2)CdSe/(8)Co^{2+}:CdS, and (2)CdSe/(10)Co^{2+}:CdS. The incorporation of Co^{2+} into the CdS shell was realized using a Co(II) acetate complex in a slightly modified c-ALD procedure as reported previously by Delikanli *et al.*[45] (see the "Methods" section for further information). The doping concentration of the CdSe/Co^{2+}:CdS NPLs in each shell layer is about 0.8% and has been determined via inductively coupled plasma atomic emission spectroscopy (ICP-AES). Undoped CdSe/CdS NPLs with identical core/shell structure were prepared as a reference. Representative transmission electron microscope images of the (2)CdSe/(8)Co^{2+}:CdS NPLs depicting the lateral dimensions (~35 nm × 45 nm) and a thickness of ~3.3 nm can be found in the supplementary material [see Figs. S1(a) and S1(b)]. While the lateral dimensions are comparable in thinner or thicker NPLs [(2)CdSe/(6)Co^{2+}:CdS and (2)CdSe/(10)Co^{2+}:CdS], each additional monolayer of the shell material corresponds to a change in the thickness of ~0.35 nm.

Figure 1(a) depicts the absorption spectra of CdSe/Co^{2+}:CdS NPLs measured in dispersion using hexane as solvent. The spectra have been normalized to the second absorption maximum observed between 520 and 550 nm. Well-defined excitonic features related to different transitions have been observed in the high energy part of the spectrum ($\lambda < 625$ nm). The valence band (VB) in II–VI-based two-dimensional (2D) materials is composed of three sub-bands (heavy hole, light hole, and split off, abbreviated hh, lh, and so, respectively) with defined hole character. A multitude of VB energy states can be defined using the nomenclature hh_n, lh_n, and so_n, with n representing the principal quantum number of the respective energy state. The energy states of the conduction band (CB) are described as e_n. The excited states of excitonic nature, which can be observed in the absorption spectra, are denoted by VB_ne_n-X. According to this model, the excited state observed at the lowest energy is related to hh_1e_1-X, observed in the samples studied here in the spectral range between 570 and 600 nm. The second (third) absorption feature observed between 520 and 550 nm (470 and 500 nm) is related to the lh_1e_1-X (so_1e_1-X) transition. A detailed assignment of these transitions based on double-potential quantum well calculations is provided elsewhere.[47] The energy redshift with increasing shell thickness is a consequence of the delocalization of the wavefunction of the charge carriers into the shell, specifically of the electron in the CB, which in turn weakens the quantum confinement.[12]

Additional absorption features with significantly smaller oscillator strength have been observed in the wavelength range between 650 and 800 nm. The inset of Fig. 1(a) depicts the absorption spectra with scaled y-axis to enable the data analysis. These features give a first hint that Co^{2+} incorporation into the CdS shell was

Published under license by AIP Publishing

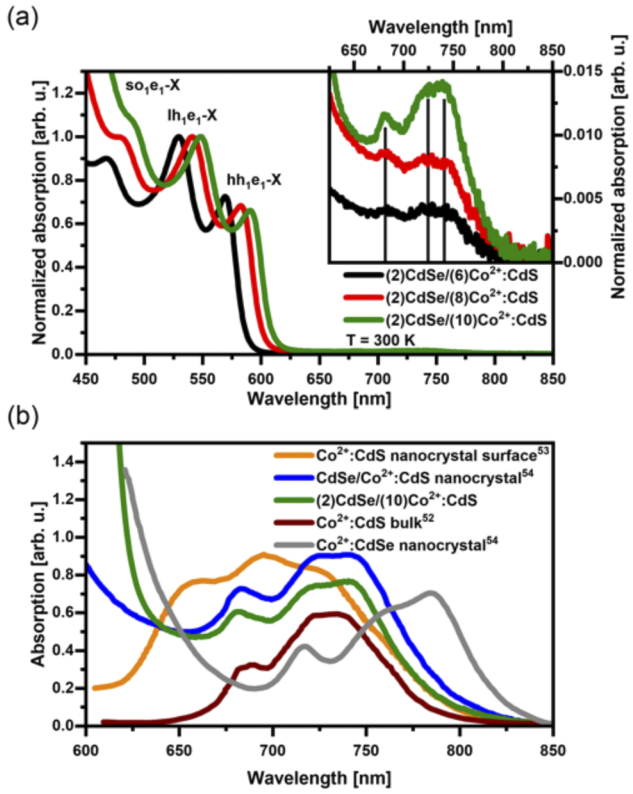

FIG. 1. (a) Normalized absorption spectra of CdSe/Co^{2+}:CdS nanoplatelets with different shell thicknesses (6, 8, and 10 monolayers, depicted in black, red, and green, respectively). Excitonic features related to different excited states (hh_1e_1-X, lh_1e_1-X, and so_1e_1-X) are observed in the high energy part of the spectrum ($\lambda < 625$ nm). Inset: Additional absorption features observed for 650 nm $< \lambda <$ 800 nm related to Co^{2+} ligand field transitions. (b) Comparison between the Co^{2+} ligand field transitions observed in CdSe/Co^{2+}:CdS NPLs coated with a 10 ML thick shell (green curve) and literature data reported for Co^{2+} LF transitions in different coordination geometries. The brown (blue) curve represents the absorption data reported for bulk Co^{2+}:CdS[52] (CdSe/Co^{2+}:CdS nanocrystals[54]). In gray, the LF transitions reported for Co^{2+}:CdSe nanocrystals[54] are shown, while the orange curve is related to LF transitions of Co^{2+} located on the surface of CdS nanocrystals.[53]

successful, since their energy range matches the expected one for ligand field (LF) transitions in Co^{2+} ions tetrahedrally coordinated by sulfur ions.[52] Moreover, the amplitude of the Co^{2+} ligand field transitions increases with increasing shell thickness. This, combined with the fact that the doping concentration in the CdS shell is similar among the different samples, is a sign that a larger number of impurities have been incorporated into NPLs with a thicker CdS shell compared to their thinner shell analogs. A representative comparison between a doped core/shell NPL and its undoped reference can be found in the supplementary material (see Fig. S2).

Since the energies of the Co^{2+} ligand field transitions strongly depend on the bonding length of these ions to their nearest neighbors, a detailed analysis of the absorption spectra enables a fundamental understanding of the dopant incorporation process. More precisely, one might get access to the diffusion of Co^{2+} impurities into the core and the presence of these ions at the interface between core and shell as well as on the shell surface. Figure 1(b) shows a comparison between the Co^{2+} LF transitions observed in our core/shell NPLs with a 10 ML thick shell (green curve, data collected on a thin film, which was fabricated by drop-casting the original NPL dispersion onto a quartz substrate) and literature data reported for LF transitions in different coordination geometries. In zinc-blende structures, Co^{2+} is tetrahedrally coordinated by four anion ligands. Thus, in order to discuss the dopant environment, we use the coordination chemistry notation $Co(\mu_4\text{-ligand})_4$. In the sample fabrication process, the precursor for dopant incorporation [cobalt(II)-acetate] is only added during the shell growth onto preformed CdSe NPLs. Therefore, it is most likely that Co^{2+} ions are incorporated into the CdS shell, having $Co(\mu_4\text{-S})_4$ coordination geometry. In the case of a significant diffusion of the Co^{2+} dopants into the CdSe core, one would expect signatures of $Co(\mu_4\text{-Se})_4$ in the absorption spectrum. The data collected in our samples are very similar to literature reports for bulk Co^{2+}:CdS [see the brown curve in Fig. 1(b)—data from Ref. 52] and CdSe/Co^{2+}:CdS nanocrystals [see the blue curve in Fig. 1(b)—data from Ref. 54]. Moreover, a strong discrepancy between our experimental data and the data for Co^{2+}:CdSe nanocrystals reported by Archer *et al.*[54] [see the gray curve in Fig. 1(b)] is obtained. These findings demonstrate controlled incorporation of Co^{2+} ions into the CdS shell, without relevant diffusion of the dopants into the CdSe core.

Due to the small shell thickness of the NPLs, one might assume that some Co^{2+} ions are present in a pseudotetrahedral coordination geometry, e.g., if Co^{2+} ions are located at the interface to the CdSe core. In this case, Co^{2+} would experience a mixed environment $[Co(\mu_4\text{-S})_{4-x}(Se)_x]$ due to the two different ligand ions (S^{2-} and Se^{2-}). Therefore, the absorption features are expected in the spectral range between the literature reports for bulk Co^{2+}:CdS[52] and Co^{2+}:CdSe nanocrystals,[54] with the precise energy depending on the exact number of each ligand type and the distortion. However, the large similarity between our experimental data and literature reports on bulk Co^{2+}:CdS[52] gives a strong hint that the replacement of cations of the Cd-rich surfaces of the core by Co^{2+} during or after the shell growth is not significant. Note that during the shell growth via c-ALD, first precursors for the incorporation of anions (here S^{2-}) are supplied, which attach to the Cd-rich surface of the core before the shell cations (Cd^{2+} and Co^{2+}, respectively) are added.

Another pseudotetrahedral coordination should be considered for Co^{2+} ions located at the oleylamine (OLA)-functionalized surface of the core/shell NPLs. In this case, $Co(\mu_4\text{-S})_{4-x}(N(OLA))_x$ is the expected coordination geometry. Radovanovic and Gamelin reported an absorption spectrum of surface-bound $Co(\mu_4\text{-S})_{4-x}(N(py))_x$,[53] indicated by the orange curve in Fig. 1(b). The surface of their nanocrystals is functionalized with pyridine (py). They observed that a mixed coordination environment at the surface of a nanostructure leads to an energy blueshift of the absorption features when compared to $Co(\mu_4\text{-S})_4$ in Co^{2+}:CdS. This is caused by the larger ligand field strength of nitrogen ions compared to sulfur ones. We have not been able to observe any features similar to the reported data on surface-bound $Co(\mu_4\text{-S})_{4-x}(N(py))_x$,

Published under license by AIP Publishing

i.e., the configuration $Co(\mu_4\text{-}S)_{4-x}(N(OLA))_x$ does not dominate the Co^{2+} LF transitions. However, since for $\lambda < 670$ nm Co^{2+} LF absorption features overlap with the hh_1e_1-X resonance, we cannot completely exclude the possibility that a small number of the Co^{2+} dopants are located at the surface of our core/shell NPLs.

As one cools the NPLs down to helium temperatures, a quantitative analysis of the energies of the LF transitions without the phonon-induced linewidth broadening present at higher temperatures becomes possible. The bottom curve in Fig. 2(a) depicts the absorption spectrum related to the Co^{2+} LF transitions in (2)CdSe/(10)Co^{2+}:CdS NPLs measured at $T = 4.3$ K. Four spectrally well-resolved absorption maxima and one additional feature related to the high-energy shoulder of the peak of the highest intensity can be identified, whose energies at $T = 4.3$ K are marked by the dashed vertical lines. In a tetrahedral field, the $^4A_2$ ground state of a d^7 ion (such as Co^{2+}) is derived from the ^4F free-ion term. The first three excited states are labeled $^4T_2(F)$, $^4T_1(F)$, and $^4T_1(P)$, the first one being the state of lowest energy (see the Tanabe-Sugano diagram in the supplementary material—Fig. S3). The Co^{2+} LF absorption bands of the lowest energies, $^4A_2 \rightarrow {}^4T_2(F)$ and $^4A_2 \rightarrow {}^4T_1(F)$, are expected in the near-infrared wavelength range, thus not being observed in our experiment. At the ligand field strength of CdS, the $^4T_1(P)$ excited state overlaps with additional states derived from the ^2G free-ion term,[55] making the assignment of the observed LF transitions in the wavelength range between 670 and 800 nm more challenging. According to the results on the optical spectra of transition metal ions on tetrahedral sites published by Weakliem,[52] we propose the following assignment of the features observed in our experimental data: between 700 and 754 nm, the absorption bands are related to different $^4A_2 \rightarrow {}^4T_1(P)$ LF transitions. The absorption feature at ~ 690 nm (678 nm) is attributed to the $^4A_2 \rightarrow {}^2A_1(G)$ ($^4A_2 \rightarrow {}^2T_2(G)$) LF transition. A possible deviation between LF energies observed in our NPLs and the low-temperature absorption data reported in bulk Co^{2+}:CdS[52,56] is within the resolution limit of our experiment.

Figure 2(a) depicts the temperature-dependent absorption spectra of the Co^{2+} LF transitions, showing that both the energy of the observed absorption features and their linewidth are impacted by the temperature. This temperature dependence is a direct consequence of the electron-phonon interaction, which has been observed in transition metal and rare earth impurities incorporated in different host lattices.[49,57–63] Similar to previous literature reports on Co^{2+} dopants in halide-based lattices,[63] the full width half maximum (FWHM) of Co^{2+} LF transition features is roughly constant in the low temperature range, while for higher temperatures, the influence of lattice vibrations leads to a significant linewidth broadening.

The energy shift of the Co^{2+} LF transitions with temperature is a consequence of the electron–phonon interaction between the lattice phonons and the electrons of the transition metal impurity. A representative fit of the data used for the extraction of the temperature-dependent energy of different absorption features can be found in the supplementary material (see Fig. S4). We extracted the energy of the Co^{2+} LF transition for all features marked by the dashed lines in Fig. 2(a). The dashed curves in Fig. 2(b) are simulations of the impact of the temperature on the energy shift δE, which have been calculated using the following theoretical expression:[64]

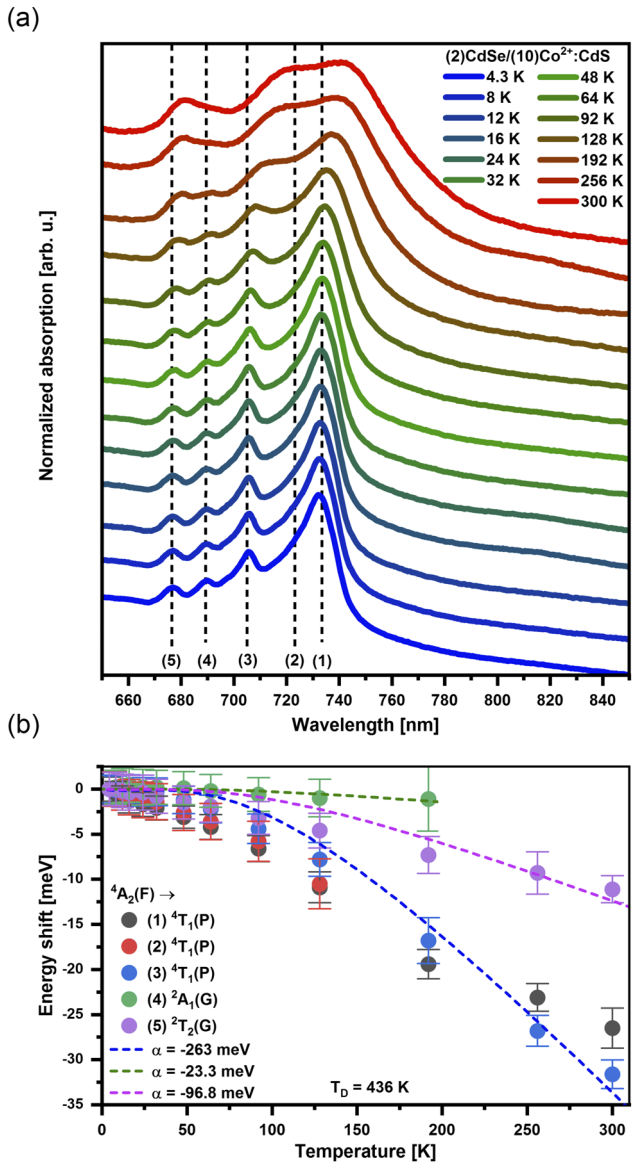

FIG. 2. (a) Normalized temperature dependent absorption spectra depicting Co^{2+} ligand field transitions in CdSe/Co^{2+}:CdS NPLs with a 10 ML thick shell. The dashed lines mark the energy position of the maxima observed at the lowest temperature (T = 4.3 K). (b) Temperature-dependent energy shift of different features observed in the absorption spectrum of Co^{2+} LF transitions [marked as dashed lines in panel (a)]. The dashed colored lines represent fits according to Eq. (1).

$$\delta E = \alpha \cdot \left(\frac{T}{T_D}\right)^4 \int_0^{T_D/T} \frac{x^3}{e^x - 1} dx, \tag{1}$$

T_D is the effective Debye temperature and $x = \hbar\omega/k_BT$, where k_B is the Boltzmann constant and $\hbar\omega$ is the phonon energy. In our simulations, we assumed $T_D = 436$ K (value reported for CdS

Published under license by AIP Publishing

nanocrystals[65]) and $\hbar\omega$ = 38 meV, which is the reported LO phonon energy for bulk CdS.[66] The constant α describes a coupling coefficient for the electron–phonon interaction, which is the only adjustable parameter.

For peaks 1–3 [$^4A_2 \rightarrow {}^4T_1(P)$], a simulation assuming $|\alpha| \sim 263$ meV matches the experimental data quite well, while for peaks 4 and 5 [$^4A_2 \rightarrow {}^2A_1(G)$ and $^4A_2 \rightarrow {}^2T_2(G)$, respectively] smaller, values for the electron-phonon coupling strength [e.g., $|\alpha| \sim 97$ meV for $^4A_2 \rightarrow {}^2T_2(G)$] are necessary to describe the observed $\delta E(T)$. It is instructive to compare these values with literature reports on transition metal doped materials. The Meijerink group investigated the electron-phonon coupling of transitions between spin-orbit split components of the $^4T_{1g}$ cubic-field ground term of Co^{2+} in cadmium halides CdX_2 (X: Cl, Br, and I),[63] extracting $|\alpha| = 13$–32 meV. The strength of the electron-phonon coupling strongly depends on the host lattice: Stronger coupling is expected in more covalent lattices[58] like the II–VI compounds studied here, justifying the larger values of $|\alpha|$ found in our experiments. An additional comparison can be drawn with results reported for the $^4T_1 \rightarrow {}^6A_1$ emission in Mn^{2+}:ZnS nanocrystals.[49] Although the authors do not explicitly report a value for α, analyzing their fits allowed us to extract a value of $|\alpha| \approx 120$ meV, which is in the same order of magnitude as the values extracted from our data.

Subsequently, we took advantage of magnetic circular dichroism (MCD) spectroscopy to investigate the magneto-optical response of the Co^{2+} impurities. The low temperature absorption and MCD data of the Co^{2+} LF transitions in (2)CdSe/(10)Co^{2+}:CdS NPLs are plotted in Fig. 3(a). The dashed lines highlight the energy positions of the absorption maxima. The total energy-dependent MCD amplitude can be described using the following equation:[67]

$$MCD(E) = A \cdot \frac{-\partial f(E)}{\partial E} + B_0 \cdot f(E) + \frac{C}{k_B T} \cdot f(E). \qquad (2)$$

Herein, $f(E)$ describes the shape of the absorption feature, while A, B_0, and C are prefactors for the different MCD terms. While $A \cdot \frac{-\partial f(E)}{\partial E}$ is a derivative-shaped term (called A-term), $B_0 \cdot f(E)$ and $\frac{C}{k_B T} \cdot f(E)$ exhibit a Gaussian line shape (called B_0- and C-term, respectively). The A-term is related to a Zeeman splitting of the excited state, shifting the absorption bands for right and left circularly polarized light with respect to each other in energy. In this case, the maximum in absorption will coincide with the MCD zero-crossing. The fact that the maxima observed in the absorption spectrum coincide with either a maximum or a minimum in the MCD signal allows us to draw the conclusion that the MCD activity is a result of either a B_0- or a C-term, excluding a dominant contribution of an A-term. The B_0-term is related to a field-induced mixing between nearby excited states, while the C-term is caused by an unequal population of the Zeeman sublevels of a paramagnetic ground state. Since the B_0-term is temperature-independent and the C-term exhibits a temperature dependence, varying the temperature enables one to determine the dominating term for the observed MCD activity of the Co^{2+} LF transitions [see Fig. 3(b)].

The temperature dependence of the Co^{2+} LF transitions in the MCD data can be explained as follows: An external magnetic field lifts the degeneracy of the Co^{2+} ground state quartet ($^4A_2$), and these states are unequally populated at low temperatures creating

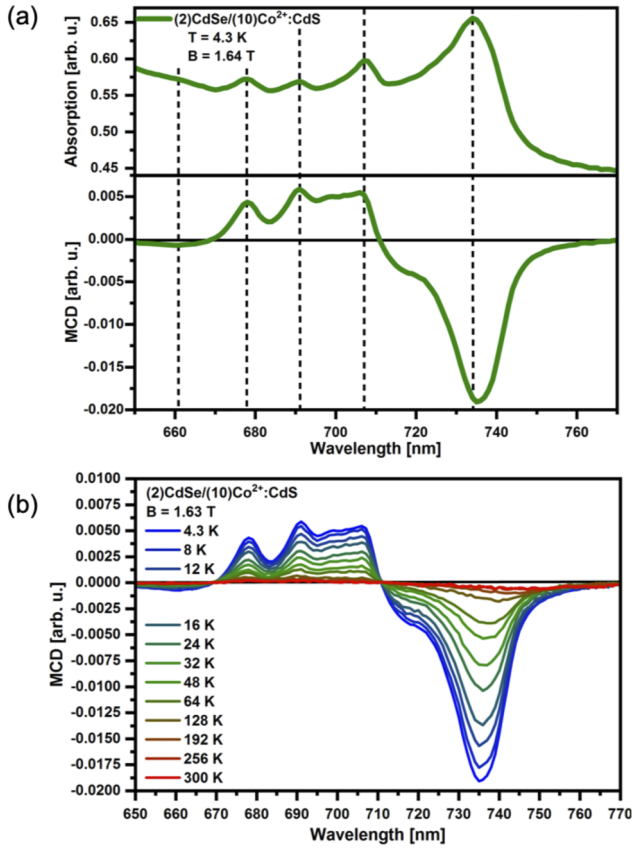

FIG. 3. (a) Absorption and MCD spectra of CdSe/Co^{2+}:CdS NPLs with a 10 ML thick shell measured at 4.3 K and B = 1.64 T. The dashed lines mark the energy position of the maxima observed in the absorption spectrum. (b) Temperature-dependent MCD spectra of Co^{2+} LF transitions of (2)CdSe/(10)Co^{2+}:CdS NPLs collected at B = 1.63 T.

a net magnetization. This unequal population leads to a different absorption strength of right and left circularly polarized light, thus resulting in a C-term MCD signal. Due to the small g-value for the $^4A_2$ state in Co^{2+} ($g = 2.26$),[68] the thermal energy k_BT exceeds the Zeeman splitting $g\mu_B B$ (~0.2 meV at B = 1.6 T) even at moderately low temperatures. Therefore, the C-term MCD amplitude is proportional to $g\mu_B B/k_B T$ (see Ref. 69 for further details), reflecting the Curie limit of the ground state magnetization of the Co^{2+} ions. As expected, the MCD amplitude of the Co^{2+} LF transitions thus decreases with increasing temperature [see Fig. 3(b)]. These results are in agreement with previous literature reports on tetrahedrally coordinated Co^{2+} ions in molecular complexes[70] and Co^{2+}-doped nanocrystals.[56]

MCD spectroscopy can also be used to investigate the *sp-d* exchange interaction between the magnetic dopants and the charge carriers of the host lattice, i.e., to probe the magneto-optical activity of excited states of excitonic nature. In the case of the *sp-d* exchange interaction, the energy splitting between the excited states in a magnetic field is expected to be significantly larger than the intrinsic Zeeman splitting present in undoped materials, thus

Published under license by AIP Publishing

leading to its denomination as giant Zeeman splitting.[73] Figure 4(a) shows the magnetic-field (B) dependent MCD data collected on (2)CdSe/(10)Co^{2+}:CdS NPLs at T = 4.3 K. In the high energy part of the spectrum (λ < 600 nm), excited states of excitonic nature (hh_1e_1-X, lh_1e_1-X, and so_1e_1-X) are observed, while at lower energies (λ > 650 nm), Co^{2+} LF transitions as discussed above are present. The correlation between the MCD amplitude of different features (excitonic nature or arising from Co^{2+} LF transitions) and the applied magnetic field can be seen in the inset of Fig. 4(a). The observed linear behavior between the MCD amplitude and the magnetic field is expected for paramagnetic systems at modest fields, i.e., below saturation. As expected, the MCD amplitude—and thus the giant Zeeman splitting—is significantly larger for hh_1e_1-X than for lh_1e_1-X due to the different strength of the exchange coupling, in agreement with Mn^{2+}-doped two-dimensional systems.[47,71] Moreover, the larger delocalization of the hole wavefunction into the doped shell for excited states of even higher energy[47] explains the fact that so_1e_1-X exhibit a large MCD amplitude.

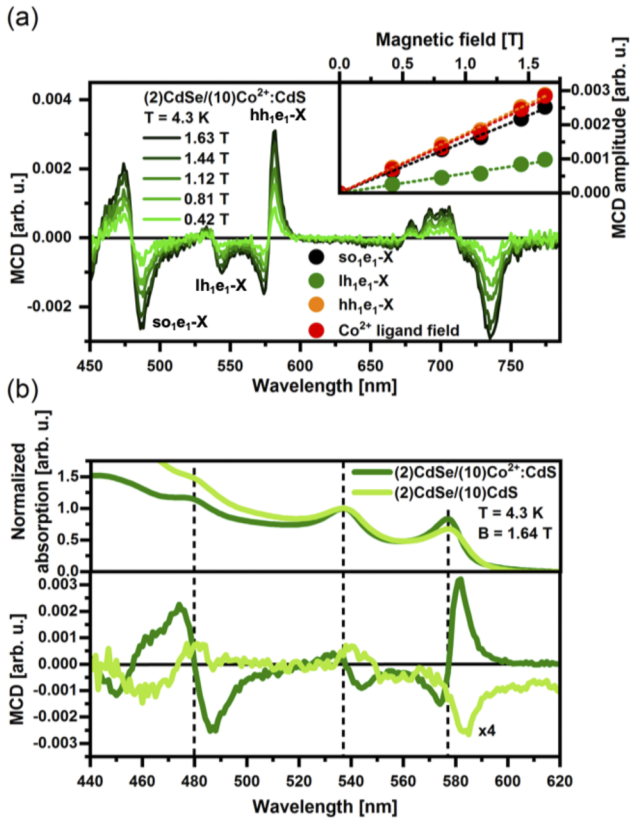

FIG. 4. (a) Magnetic field dependent MCD spectra of (2)CdSe/(10)Co^{2+}:CdS NPLs. Inset: Magnetic-field dependent amplitude of hh_1e_1-X (orange), lh_1e_1-X (green), so_1e_1-X (black) excited states and Co^{2+} LF transitions (red) extracted from the data plotted in the main panel. (b) Absorption (top) and MCD spectra of undoped (light green) and CdSe/Co^{2+}:CdS NPLs with a 10 ML thick shell (green) measured at 4.3 K. The dashed lines mark the energy position of the maxima observed in the absorption spectrum. The MCD of the undoped reference has been multiplied by a factor of 4 to facilitate the comparison.

Figure 4(b) depicts the absorption (top panel) and MCD spectra of (2)CdSe/(10)Co^{2+}:CdS NPLs (green) and of the undoped reference [(2)CdSe/(10)CdS—light green]. Data collected on (2)CdSe/(8)Co^{2+}:CdS NPLs and their undoped reference [(2)CdSe/(8)CdS] can be found in the supplementary material (see Fig. S5). The dashed lines mark the energy position of the maxima observed in the absorption spectrum, showing that the maximum in absorption indeed coincides with the MCD zero-crossing, as expected for an A-term MCD signature. While the absorption spectra of the doped and of the undoped NPLs look very similar, their MCD spectra are quite distinct. Not only the amplitude of the MCD signal is at least 5 times larger in the case of the doped NPLs compared to their undoped analogs, also a sign change for hh_1e_1-X MCD resonance could be observed. The g-factors related to the intrinsic Zeeman splitting of the first excited state exhibit positive sign for both bulk and 2D chalcogenide-based lattices.[72–74] Additionally, it has been shown that in the case of pronounced *sp-d* exchange interaction, the g-factor of the hh_1e_1-X state in 2D nanocrystals changes its sign.[47] Therefore, the observation of a sign change in the MCD signal upon doping is a hint that magnetic exchange interactions between the incorporated Co^{2+} ions and the charge carriers of the host lattice take place.

To get further insight into the magneto-optical response of excitonic states, we additionally conducted temperature-dependent MCD experiments. Figure 5(a) depicts the temperature-dependent behavior of the MCD signal from T = 4.3 K to 300 K. Additional data collected on (2)CdSe/(8)Co^{2+}:CdS and (2)CdSe/(6)Co^{2+}:CdS NPLs show similar behavior and can be found in the supplementary material (see Fig. S6).

In the case of *sp-d* exchange interactions between the host charge carriers and the magnetic dopants, the MCD signal is expected to be proportional to the magnetization of the Co^{2+} ions, with a temperature dependence according to the Brillouin function.[75,76] For a constant magnetic field (in our case B = 1.64 T), the magnetization of a paramagnetic system decreases as the temperature increases due to thermal disorder. We observed a temperature-induced decrease in the MCD amplitude for all observed excitonic transitions, following the behavior expected for paramagnetic systems.

To enable the analysis of the temperature dependent behavior of the different transitions, their MCD amplitudes have been normalized to the maximum value measured at T = 4.3 K and plotted vs temperature. Figure 5(b) depicts the data extracted for the excitonic transitions. In the case of hh_1e_1-X, the MCD amplitude drops with increasing temperature and the sign of the MCD signal swaps at T = 48 K. Such a behavior has been previously observed for the excited state of lowest energy in CdSe nanocrystals with extreme low Mn^{2+} content and explained by the competition between (temperature-independent) intrinsic and (temperature-dependent) giant Zeeman splitting, which exhibit opposite sign.[77,78] It is important to note that the modest magneto-optical response observed is caused by both the low Co^{2+} content and the small overlap γ between the charge carrier wavefunctions and the dopants due to the core/shell structure. Both, lh_1e_1-X and so_1e_1-X exhibit opposite sign compared to the data of hh_1e_1-X for T < 48 K. The deviation between hh_1e_1-X (and lh_1e_1-X) and the Brillouin fit can be explained by the competition between giant and intrinsic Zeeman splittings. Figure 5(c) depicts the data extracted for the Co^{2+} ligand field

Published under license by AIP Publishing

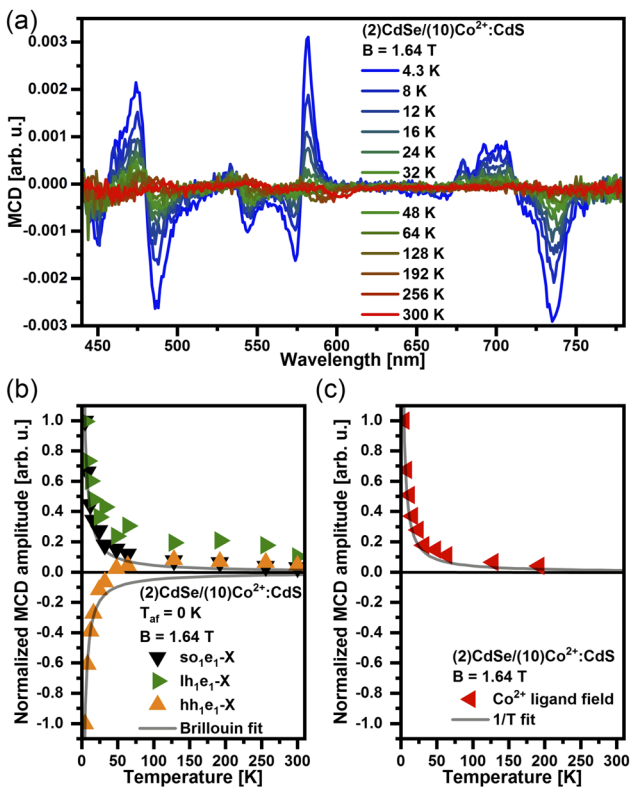

FIG. 5. (a) Temperature-dependent MCD spectra of (2)CdSe/(10)Co^{2+}:CdS NPLs collected at B = 1.64 T. (b) Normalized MCD amplitude of hh_1e_1-X (orange), lh_1e_1-X (green) and so_1e_1-X (black) transition. The gray curves represent Brillouin fits. (c) Normalized MCD amplitude of the Co^{2+} ligand field transitions (red) extracted from the data plotted in panel (a). The solid line represents the expected behavior of a pure paramagnetic system in the Curie limit of $k_BT \gg g\mu_BB$.

transitions. The MCD amplitude for a pure paramagnetic spin ensemble with $S = 3/2$ in the case of $k_BT \gg g\mu_BB$ is expected to be proportional to $1/T$ (see gray curves). It is clear that the $1/T$-dependence fits well the observed temperature-induced decrease in the MCD amplitude of the Co^{2+} ligand field transitions.

CONCLUSIONS

In summary, temperature dependent absorption and MCD spectroscopy were used to investigate the incorporation of Co^{2+} into the shell material in CdSe/CdS NPLs of different shell thicknesses. In the high energy range ($\lambda < 620$ nm) of the absorption spectra, excited states of excitonic nature have been observed, while at longer wavelengths (670 nm $< \lambda <$ 800 nm), the absorption bands are related to interatomic Co^{2+} LF transitions. Comparing the absorption of Co^{2+} LF transitions with literature reports leads to the conclusion that Co^{2+} ions are tetrahedrally coordinated by S^{2-}, showing that diffusion of the impurities into the core during the c-ALD shell growth process, dopant incorporation on the shell surface, or even segregation of impurities can be neglected. MCD spectroscopy has been applied to successfully prove *sp-d* exchange interactions between Co^{2+} and the host lattice, evidenced by the sign change in the MCD features comparing doped NPLs and undoped analogs and by the characteristic temperature dependence of the MCD amplitude.

METHODS

Sample preparation

2 ML CdSe NPLs were used as cores in this study, and we followed a previously published procedure[79] with slight modifications for the synthesis of 2 ML core CdSe NPLs as described. For the synthesis of the cores, first 55 ml of octadecene, 1 ml of oleic acid, and 840 mg of cadmium acetate dihydrate were placed into a flask and kept under vacuum for 30 min. Then, the temperature was raised to 110 °C under nitrogen gas flow and 2 ml of 1M TOP-Se solution was added swiftly. The reaction was quenched after 2 h and the NPLs were precipitated by centrifugation after the addition of hexane and ethanol. 2 ml CdSe NPLs were dispersed in hexane and this cleaning step was repeated 3 more times to remove the unreacted precursors.

For the growth of Co^{2+} doped CdS shell layers on core 2 ML CdSe NPLs, we modified a previously reported procedure from the literature.[45,80] For the deposition of the first sulfur shell layer, CdSe NPLs dispersed in 4 ML of hexane were injected into a solution which contains 5 ml of N-methylformamide (NMF) and 80 μl of ammonium sulphide under vigorous stirring. After 2 min, NPLs were precipitated by centrifugation after the addition of toluene and acetone. The precipitated NPLs were dispersed in 5 ml of NMF, and this cleaning procedure was performed twice more for the elimination of surplus sulfur precursors. Then, the NPLs dispersed in NMF were injected into a solution which contains 0.5 ml NMF including 0.3M of cadmium acetate dihydrate and 0.1M of cobalt acetate under vigorous stirring. After 45 min, NPLs were precipitated by centrifugation after the addition of toluene and acetone. The precipitated NPLs were dispersed in 5 ml of NMF, and this cleaning procedure was performed twice more for the elimination of surplus precursors. This process of shell growth can be performed as many times as wanted. Likewise, a CdS shell can be grown on CdSe NPLs by employing 0.3M cadmium acetate dihydrate solution.

The doping concentration in the Co^{2+} doped NPLs was obtained via ICP-MS measurements. First, the doping concentration in Co^{2+} doped NPLs for every consecutive sample grown by the c-ALD technique was obtained by using the ICP-MS results of the Co^{2+} and Cd^{2+} cations. We then calculated the Co^{2+} doping concentration in the shell by taking into account the fact that every layer holds same amounts of cations as a result of their 2D planar geometry.

MCD and absorption spectroscopy

For temperature-dependent experiments, a NPL thin film was prepared by dropcasting the dispersion onto a quartz glass substrate. The samples were placed into a helium vapor cryostat (ST-300, Janis). Absorption spectra were taken inserting the cryostat into a UV-2550 UV-VIS spectrometer (Shimadzu). MCD experiments were carried out in our homemade setup. The wavelength-tunable light source is based on a 50 W xenon lamp and a monochromator (LOT Oriel omni-λ 150, 1200 grooves/mm grating blazed at

Published under license by AIP Publishing

500 nm). The modulation between right and left circularly polarized light at a frequency of 50 kHz is realized using a combination of a linear polarizer and a photoelastic modulator (PEM-90, Hinds Instruments). The cryostat (ST-300, Janis) is placed between two poles of an electromagnet (EM4-HVA, Lake Shore) in Faraday geometry and a photomultiplier (R928, Hamamatsu) detects the transmitted light. The dc (ac) component of the optical signal is read out using an HP 34401A multimeter (lock-in amplifier Signal Recovery 7225 DSP).

SUPPLEMENTARY MATERIAL

See the supplementary material for TEM images of the Co^{2+}-doped NPLs, absorption spectra of undoped reference samples, a Tanabe-Sugano diagram for a Co^{2+} ion in a tetrahedral geometry, Co^{2+} ligand field transitions fitted by Lorentzian-shaped peaks, MCD data for undoped reference samples, and additional temperature dependent MCD data for Co^{2+}-doped NPLs with different shell thicknesses.

ACKNOWLEDGMENTS

R.F. and G.B. acknowledge the Deutsche Forschungsgemeinschaft (DFG) under Contract No. BA 1422/16-1.

REFERENCES

[1] S. Ithurria and B. Dubertret, "Quasi 2D colloidal CdSe platelets with thicknesses controlled at the atomic level," J. Am. Chem. Soc. **130**(49), 16504–16505 (2008).
[2] S. Ithurria, M. D. Tessier, B. Mahler, R. P. S. M. Lobo, B. Dubertret, and A. L. Efros, "Colloidal nanoplatelets with two-dimensional electronic structure," Nat. Mater. **10**(12), 936–941 (2011).
[3] M. D. Tessier, C. Javaux, I. Maksimovic, V. Loriette, and B. Dubertret, "Spectroscopy of single CdSe nanoplatelets," ACS Nano **6**(8), 6751–6758 (2012).
[4] C. Bouet, M. D. Tessier, S. Ithurria, B. Mahler, B. Nadal, and B. Dubertret, "Flat colloidal semiconductor nanoplatelets," Chem. Mater. **25**(8), 1262–1271 (2013).
[5] A. Yeltik, S. Delikanli, M. Olutas, Y. Kelestemur, B. Guzelturk, and H. V. Demir, "Experimental determination of the absorption cross-section and molar extinction coefficient of colloidal CdSe nanoplatelets," J. Phys. Chem. C **119**(47), 26768–26775 (2015).
[6] A. W. Achtstein, A. Antanovich, A. Prudnikau, R. Scott, U. Woggon, and M. Artemyev, "Linear absorption in CdSe nanoplates: Thickness and lateral size dependency of the intrinsic absorption," J. Phys. Chem. C **119**(34), 20156–20161 (2015).
[7] M. Nasilowski, B. Mahler, E. Lhuillier, S. Ithurria, and B. Dubertret, "Two-dimensional colloidal nanocrystals," Chem. Rev. **116**(18), 10934–10982 (2016).
[8] R. Scott, J. Heckmann, A. V. Prudnikau, A. Antanovich, A. Mikhailov, N. Owschimikow, M. Artemyev, J. I. Climente, U. Woggon, N. B. Grosse *et al.*, "Directed emission of CdSe nanoplatelets originating from strongly anisotropic 2D electronic structure," Nat. Nanotechnol. **12**(12), 1155–1160 (2017).
[9] D. Norris, A. Efros, M. Rosen, and M. Bawendi, "Size dependence of exciton fine structure in CdSe quantum dots," Phys. Rev. B **53**(24), 16347–16354 (1996).
[10] *Semiconductor Nanocrystal Quantum Dots*, edited by A. L. Rogach (Springer Vienna, Vienna, 2008).
[11] *Nanocrystal Quantum Dots*, 2nd ed., edited by V. I. Klimov (CRC Press, Boca Raton, FL, USA, 2010).
[12] S. Ithurria and D. V. Talapin, "Colloidal atomic layer deposition (c-ALD) using self-limiting reactions at nanocrystal surface coupled to phase transfer between polar and nonpolar media," J. Am. Chem. Soc. **134**(45), 18585–18590 (2012).
[13] B. Mahler, B. Nadal, C. Bouet, G. Patriarche, and B. Dubertret, "Core/shell colloidal semiconductor nanoplatelets," J. Am. Chem. Soc. **134**(45), 18591–18598 (2012).
[14] M. D. Tessier, P. Spinicelli, D. Dupont, G. Patriarche, S. Ithurria, and B. Dubertret, "Efficient exciton concentrators built from colloidal core/crown CdSe/CdS semiconductor nanoplatelets," Nano Lett. **14**(1), 207–213 (2014).
[15] Y. Kelestemur, M. Olutas, S. Delikanli, B. Guzelturk, M. Z. Akgul, and H. V. Demir, "Type-II colloidal quantum wells: CdSe/CdTe core/crown heteronanoplatelets," J. Phys. Chem. C **119**(4), 2177–2185 (2015).
[16] S. Pedetti, S. Ithurria, H. Heuclin, G. Patriarche, and B. Dubertret, "Type-II CdSe/CdTe core/crown semiconductor nanoplatelets," J. Am. Chem. Soc. **136**(46), 16430–16438 (2014).
[17] S. Delikanli, B. Guzelturk, P. L. Hernández-Martínez, T. Erdem, Y. Kelestemur, M. Olutas, M. Z. Akgul, and H. V. Demir, "Continuously tunable emission in inverted type-I CdS/CdSe core/crown semiconductor nanoplatelets," Adv. Funct. Mater. **25**(27), 4282–4289 (2015).
[18] A. Polovitsyn, Z. Dang, J. L. Movilla, B. Martín-García, A. H. Khan, G. H. V. Bertrand, R. Brescia, and I. Moreels, "Synthesis of air-stable CdSe/ZnS core–shell nanoplatelets with tunable emission wavelength," Chem. Mater. **29**(13), 5671–5680 (2017).
[19] M. D. Tessier, B. Mahler, B. Nadal, H. Heuclin, S. Pedetti, and B. Dubertret, "Spectroscopy of colloidal semiconductor core/shell nanoplatelets with high quantum yield," Nano Lett. **13**(7), 3321–3328 (2013).
[20] Z. Chen, B. Nadal, B. Mahler, H. Aubin, and B. Dubertret, "Quasi-2D colloidal semiconductor nanoplatelets for narrow electroluminescence," Adv. Funct. Mater. **24**(3), 295–302 (2014).
[21] F. Zhang, S. Wang, L. Wang, Q. Lin, H. Shen, W. Cao, C. Yang, H. Wang, L. Yu, Z. Du *et al.*, "Super color purity green quantum dot light-emitting diodes fabricated by using CdSe/CdS nanoplatelets," Nanoscale **8**(24), 12182–12188 (2016).
[22] U. Giovanella, M. Pasini, M. Lorenzon, F. Galeotti, C. Lucchi, F. Meinardi, S. Luzzati, B. Dubertret, and S. Brovelli, "Efficient solution-processed nanoplatelet-based light-emitting diodes with high operational stability in air," Nano Lett. **18**(6), 3441–3448 (2018).
[23] B. Guzelturk, Y. Kelestemur, M. Olutas, S. Delikanli, and H. V. Demir, "Amplified spontaneous emission and lasing in colloidal nanoplatelets," ACS Nano **8**(7), 6599–6605 (2014).
[24] Z. Yang, M. Pelton, I. Fedin, D. V. Talapin, and E. Waks, "A room temperature continuous-wave nanolaser using colloidal quantum wells," Nat. Commun. **8**(1), 143 (2017).
[25] Y. Gao, M. Li, S. Delikanli, H. Zheng, B. Liu, C. Dang, T. C. Sum, and H. V. Demir, "Low-threshold lasing from colloidal CdSe/CdSeTe core/alloyed-crown type-II heteronanoplatelets," Nanoscale **10**(20), 9466–9475 (2018).
[26] J. F. Suyver, S. F. Wuister, J. J. Kelly, and A. Meijerink, "Luminescence of nanocrystalline ZnSe:Mn^{2+}," Phys. Chem. Chem. Phys. **2**(23), 5445–5448 (2000).
[27] D. J. Norris, N. Yao, F. T. Charnock, and T. A. Kennedy, "High-quality manganese-doped ZnSe nanocrystals," Nano Lett. **1**(1), 3–7 (2001).
[28] R. Beaulac, L. Schneider, P. I. Archer, G. Bacher, and D. R. Gamelin, "Light-induced spontaneous magnetization in doped colloidal quantum dots," Science **325**(5943), 973–976 (2009).
[29] H. Chen, S. Maiti, and D. H. Son, "Doping location-dependent energy transfer dynamics in Mn-doped CdS/ZnS nanocrystals," ACS Nano **6**(1), 583–591 (2012).
[30] A. Pandey, S. Brovelli, R. Viswanatha, L. Li, J. M. Pietryga, V. I. Klimov, and S. A. Crooker, "Long-lived photoinduced magnetization in copper-doped ZnSe-CdSe core-shell nanocrystals," Nat. Nanotechnol. **7**(12), 792–797 (2012).
[31] Z. Hu, S. Xu, X. Xu, Z. Wang, Z. Wang, C. Wang, and Y. Cui, "Co-doping of Ag into Mn:ZnSe quantum dots: Giving optical filtering effect with improved monochromaticity," Sci. Rep. **5**(1), 14817 (2015).
[32] K. E. Knowles, K. H. Hartstein, T. B. Kilburn, A. Marchioro, H. D. Nelson, P. J. Whitham, and D. R. Gamelin, "Luminescent colloidal semiconductor nanocrystals containing copper: Synthesis, photophysics, and applications," Chem. Rev. **116**(18), 10820–10851 (2016).
[33] H. D. Nelson, S. O. M. Hinterding, R. Fainblat, S. E. Creutz, X. Li, and D. R. Gamelin, "Mid-gap states and normal vs inverted bonding in luminescent Cu^{+}-

Published under license by AIP Publishing

and Ag^{+}-doped CdSe nanocrystals," J. Am. Chem. Soc. **139**(18), 6411–6421 (2017).
[34]N. Pradhan, S. Das Adhikari, A. Nag, and D. D. Sarma, "Luminescence, plasmonic, and magnetic properties of doped semiconductor nanocrystals," Angew. Chem., Int. Ed. **56**(25), 7038–7054 (2017).
[35]C. Pu, X. Peng, Z. Xu, X. Yang, S. Liu, and H. Qin, "Temperature- and Mn^{2+} concentration-dependent emission properties of Mn^{2+}-doped ZnSe nanocrystals," J. Am. Chem. Soc. **141**, 2288–2298 (2019).
[36]J. Eilers, E. Groeneveld, C. de Mello Donegá, and A. Meijerink, "Optical properties of Mn-doped ZnTe magic size nanocrystals," J. Phys. Chem. Lett. **3**(12), 1663–1667 (2012).
[37]J. Yang, R. Fainblat, S. G. Kwon, F. Muckel, J. H. Yu, H. Terlinden, B. H. Kim, D. Iavarone, M. K. Choi, I. Y. Kim *et al.*, "Route to the smallest doped semiconductor: Mn^{2+}-doped $(CdSe)_{13}$ clusters," J. Am. Chem. Soc. **137**(40), 12776–12779 (2015).
[38]S. Pittala, M. J. Mortelliti, F. Kato, and K. R. Kittilstved, "Substitution of Co^{2+} ions into CdS-based molecular clusters," Chem. Commun. **51**(96), 17096–17099 (2015).
[39]F. Muckel, J. Yang, S. Lorenz, W. Baek, H. Chang, T. Hyeon, G. Bacher, and R. Fainblat, "Digital doping in magic-sized CdSe clusters," ACS Nano **10**(7), 7135–7141 (2016).
[40]J. Yang, F. Muckel, W. Baek, R. Fainblat, H. Chang, G. Bacher, and T. Hyeon, "Chemical synthesis, doping, and transformation of magic-sized semiconductor alloy nanoclusters," J. Am. Chem. Soc. **139**(19), 6761–6770 (2017).
[41]J. Yang, F. Muckel, B. K. Choi, S. Lorenz, I. Y. Kim, J. Ackermann, H. Chang, T. Czerney, V. S. Kale, S.-J. Hwang *et al.*, "Co^{2+}-doping of magic-sized CdSe clusters: Structural insights via ligand field transitions," Nano Lett. **18**(11), 7350–7357 (2018).
[42]M. Sharma, K. Gungor, A. Yeltik, M. Olutas, B. Guzelturk, Y. Kelestemur, T. Erdem, S. Delikanli, J. R. McBride, and H. V. Demir, "Near-unity emitting copper-doped colloidal semiconductor quantum wells for luminescent solar concentrators," Adv. Mater. **29**(30), 1700821 (2017).
[43]M. Dufour, E. Izquierdo, C. Livache, B. Martinez, M. G. Silly, T. Pons, E. Lhuillier, C. Delerue, and S. Ithurria, "Doping as a strategy to tune color of 2D colloidal nanoplatelets," ACS Appl. Mater. Interfaces **11**(10), 10128–10134 (2019).
[44]A. H. Khan, V. Pinchetti, I. Tanghe, Z. Dang, B. Martín-García, Z. Hens, D. Van Thourhout, P. Geiregat, S. Brovelli, and I. Moreels, "Tunable and efficient red to near-infrared photoluminescence by synergistic exploitation of core and surface silver doping of CdSe nanoplatelets," Chem. Mater. **31**(4), 1450–1459 (2019).
[45]S. Delikanli, M. Z. Akgul, J. R. Murphy, B. Barman, Y. Tsai, T. Scrace, P. Zhang, B. Bozok, P. L. Hernández-Martínez, J. Christodoulides *et al.*, "Mn^{2+}-doped CdSe/CdS core/multishell colloidal quantum wells enabling tunable carrier–dopant exchange interactions," ACS Nano **9**(12), 12473–12479 (2015).
[46]J. R. Murphy, S. Delikanli, T. Scrace, P. Zhang, T. Norden, T. Thomay, A. N. Cartwright, H. V. Demir, and A. Petrou, "Time-resolved photoluminescence study of CdSe/CdMnS/CdS core/multi-shell nanoplatelets," Appl. Phys. Lett. **108**(24), 242406 (2016).
[47]F. Muckel, S. Delikanli, P. L. Hernández-Martínez, T. Priesner, S. Lorenz, J. Ackermann, M. Sharma, H. V. Demir, and G. Bacher, "Sp–d exchange interactions in wave function engineered colloidal CdSe/Mn:CdS hetero-nanoplatelets," Nano Lett. **18**(3), 2047–2053 (2018).
[48]B. Henderson and G. F. Imbusch, *Optical Spectroscopy of Inorganic Solids* (Oxford University Press, New York, 1989).
[49]J. F. Suyver, J. J. Kelly, and A. Meijerink, "Temperature-induced line broadening, line narrowing and line shift in the luminescence of nanocrystalline ZnS:Mn^{2+}," J. Lumin. **104**(3), 187–196 (2003).
[50]J. G. Solé, L. E. Bausá, and D. Jaque, *An Introduction to the Optical Spectroscopy of Inorganic Solids* (John Wiley & Sons, Ltd., Chichester, UK, 2005).
[51]B. N. Figgis and M. A. Hitchman, *Ligand Field Theory and Its Applications* (Wiley, New York, NY, USA, 2000).
[52]H. A. Weakliem, "Optical spectra of Ni^{2+}, Co^{2+}, and Cu^{2+} in tetrahedral sites in crystals," J. Chem. Phys. **36**(8), 2117–2140 (1962).
[53]P. V. Radovanovic and D. R. Gamelin, "Electronic absorption spectroscopy of cobalt ions in diluted magnetic semiconductor quantum dots: Demonstration of an isocrystalline core/shell synthetic method," J. Am. Chem. Soc. **123**(49), 12207–12214 (2001).
[54]P. I. Archer, S. A. Santangelo, and D. R. Gamelin, "Inorganic cluster syntheses of TM^{2+}-doped quantum dots (CdSe, CdS, CdSe/CdS): Physical property dependence on dopant locale," J. Am. Chem. Soc. **129**(31), 9808–9818 (2007).
[55]Y. Tanabe and S. Sugano, "On the absorption spectra of complex ions II," J. Phys. Soc. Jpn. **9**(5), 766–779 (1954).
[56]P. R. Radovanovic and D. R. Gamelin, "Magnetic circular dichroism spectroscopy of Co^{2+}:CdS diluted magnetic semiconductor quantum dots," Proc. SPIE **4809**, 51–61 (2002).
[57]D. E. Mccumber and M. D. Sturge, "Linewidth and temperature shift of the R lines in ruby," J. Appl. Phys. **34**(6), 1682–1684 (1963).
[58]A. Meijerink, G. Blasse, J. Sytsma, C. de Mello Donega, and A. Ellens, "Electron-phonon coupling in rare earth compounds," Acta Phys. Pol., A **90**(1), 109–119 (1996).
[59]A. Ellens, H. Andres, A. Meijerink, and G. Blasse, "Spectral-line-broadening study of the trivalent lanthanide-ion series. I. Line broadening as a probe of the electron-phonon coupling strength," Phys. Rev. B **55**(1), 173–179 (1997).
[60]D. K. Sardar and S. C. Stubblefield, "Temperature dependencies of linewidths, positions, and line shifts of spectral transitions of trivalent neodymium ions in barium magnesium yttrium germanate laser host," J. Appl. Phys. **83**(3), 1195–1199 (1998).
[61]Z. Liu, B. Qu, J. L. Doualan, B. Xu, H. Xu, Z. Cai, A. Braud, P. Camy, and R. Moncorgé, "Temperature effects on the main absorption and emission lines of the Pr^{3+}:$LiYF_4$ laser crystal," J. Opt. Soc. Am. B **32**(2), 263 (2015).
[62]A. Vink and A. Meijerink, "Electron–phonon coupling of Cr^{3+} in YAG and YGG," J. Lumin. **87-89**, 601–604 (2000).
[63]A. P. Vink, A. Meijerink, and G. D. Jones, "Temperature dependence of infrared-absorption lines of Co^{2+} in cadmium halides," Phys. Rev. B **66**(13), 134303 (2002).
[64]X. Chen, Y. Liu, and D. Tu, *Lanthanide-Doped Luminescent Nanomaterials* (Springer Berlin Heidelberg, Berlin, Heidelberg, 2014).
[65]J. Rockenberger, L. Tröger, A. L. Rogach, M. Tischer, M. Grundmann, A. Eychmüller, and H. Weller, "The contribution of particle core and surface to strain, disorder and vibrations in thiolcapped CdTe nanocrystals," J. Chem. Phys. **108**(18), 7807–7815 (1998).
[66]O. Madelung, *Semiconductors: Data Handbook*, 3rd ed. (Springer-Verlag, Berlin, 2003).
[67]W. R. Mason, *A Practical Guide to Magnetic Circular Dichroism Spectroscopy* (John Wiley & Sons, Inc., Hoboken, NJ, USA, 2007).
[68]U. Gennser, X. C. Liu, T. Q. Vu, D. Heiman, T. Fries, Y. Shapira, M. Demianiuk, and A. Twardowski, "Exchange energies, bound magnetic polarons, and magnetization in CdSe:Co and CdS:Co," Phys. Rev. B **51**(15), 9606–9611 (1995).
[69]A. D. Buckingham and P. J. Stephens, "Magnetic optical activity," Annu. Rev. Phys. Chem. **17**(1), 399–432 (1966).
[70]T. A. Kaden and B. Holmquist, "Magnetic circular dichroism of cobalt(II) complexes," Inorg. Chem. **13**(11), 2585–2590 (1974).
[71]R. Fainblat, J. Frohleiks, F. Muckel, J. H. Yu, J. Yang, T. Hyeon, and G. Bacher, "Quantum confinement-controlled exchange coupling in manganese(II)-doped CdSe two-dimensional quantum well nanoribbons," Nano Lett. **12**(10), 5311–5317 (2012).
[72]M. Kuno, M. Nirmal, M. G. Bawendi, A. Efros, and M. Rosen, "Magnetic circular dichroism study of CdSe quantum dots," J. Chem. Phys. **108**(10), 4242 (1998).
[73]J. A. Gaj, in *Introduction to the Physics of Diluted Magnetic Semiconductors*, Springer Series in Materials Science Vol. 144, edited by J. A. Gaj and J. Kossut (Springer Berlin Heidelberg, Berlin, 2010).
[74]E. V. Shornikova, L. Biadala, D. R. Yakovlev, D. Feng, V. F. Sapega, N. Flipo, A. A. Golovatenko, M. A. Semina, A. V. Rodina, A. A. Mitioglu *et al.*, "Electron and hole G-factors and spin dynamics of negatively charged excitons in CdSe/CdS colloidal nanoplatelets with thick shells," Nano Lett. **18**(1), 373–380 (2018).
[75]C. Rigaux, "Magnetooptics in narrow gap diluted magnetic semiconductors," in *Semiconductors and Semimetals*, edited by J. K. Furdyna and J. Kossut (Elsevier, 1988), Chap. 6, Vol. 25, pp. 229–274.

Published under license by AIP Publishing

[76]J. A. Gaj and J. Kossut, "Basic consequences of sp-d and d-d interactions in DMS," in *Introduction to the Physics of Diluted Magnetic Semiconductors*, edited by J. Kossut and J. A. Gaj (Springer-Verlag, Berlin, 2010), pp. 1–36.
[77]A. M. Schimpf and D. R. Gamelin, "Thermal tuning and inversion of excitonic Zeeman splittings in colloidal doped CdSe quantum dots," J. Phys. Chem. Lett. **3**(10), 1264–1268 (2012).
[78]C. J. Barrows, R. Fainblat, and D. R. Gamelin, "Excitonic Zeeman splittings in colloidal CdSe quantum dots doped with single magnetic impurities," J. Mater. Chem. C **5**(21), 5232–5238 (2017).
[79]S. Delikanli, G. Yu, A. Yeltik, S. Bose, T. Erdem, J. Yu, O. Erdem, M. Sharma, V. K. Sharma, U. Quliyeva *et al.*, "Ultrathin highly luminescent two-monolayer colloidal CdSe nanoplatelets," Adv. Funct. Mater. **29**(35), 1901028 (2019).
[80]R. Strassberg, S. Delikanli, Y. Barak, J. Dehnel, A. Kostadinov, G. Maikov, P. L. Hernandez-Martinez, M. Sharma, H. V. Demir, and E. Lifshitz, "Persuasive evidence for electron–nuclear coupling in diluted magnetic colloidal nanoplatelets using optically detected magnetic resonance spectroscopy," J. Phys. Chem. Lett. **10**(15), 4437–4447 (2019).

Published under license by AIP Publishing